Electronic supplementary information (ESI) for

Preparation of Dihydroquinazoline Carbohydrazone Fe(II) Complexes for Spin Crossover

Fu-Xing Shen,[a] Wei Huang,*[a] Takashi Yamamoto,[b] Yasuaki Einaga,[b] Dayu Wu[a]*

[a]*Jiangsu Key Laboratory of Advanced Catalytic Materials and Technology, Collaborative Innovation Center of Advanced Catalysis & Green Manufacturing, School of Petrochemical Engineering, Changzhou University, Jiangsu 213164, China; Email: wudy@cczu.edu.cn.*
[b]*Department of Chemistry, Faculty of Science and Technology, Keio University, 3-14-1 Hiyoshi, Yokohama, 223-8522, Japan.*

1. NMR Spectroscopy

2-(pyridin-2-yl)-3-((pyridin-2-ylmethylene)amino)-2,3-dihydroquinazolin-4(1H)-one

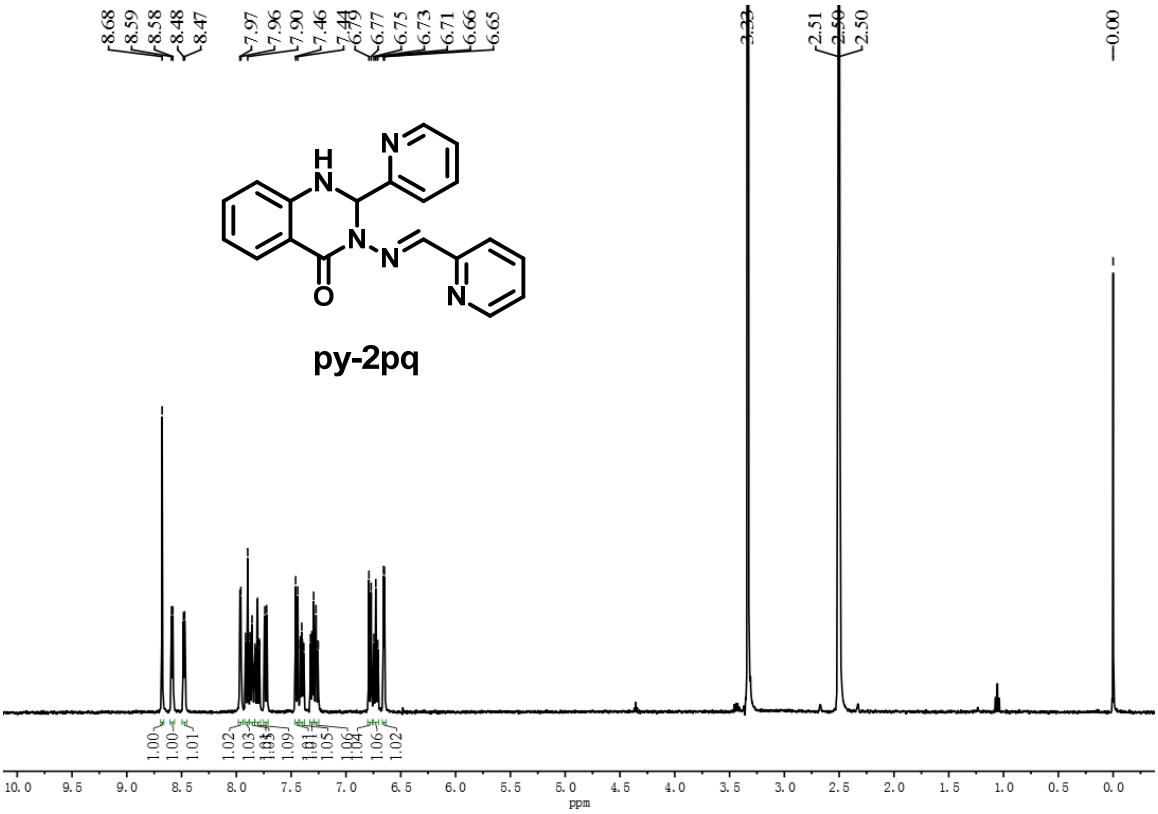

Figure S1. ^{1}H NMR spectrum of **pq-2py** in DMSO.

2-amino-N'-(pyridin-2-ylmethylene)benzohydrazide

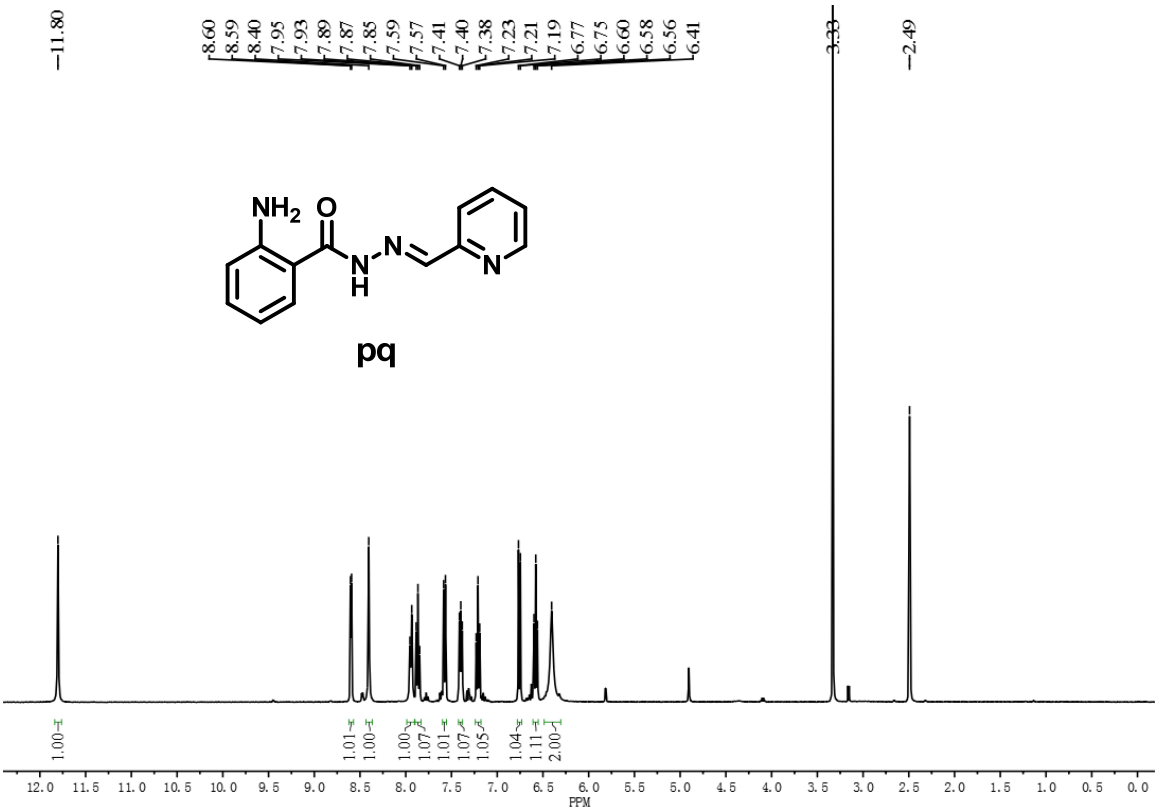

Figure S2. ^{1}HNMR spectrum of **pq** in DMSO.

2-(2-methoxyphenyl)-3-((pyridin-2-ylmethylene)amino)-2,3-dihydroquinazolin-4(1H)-one

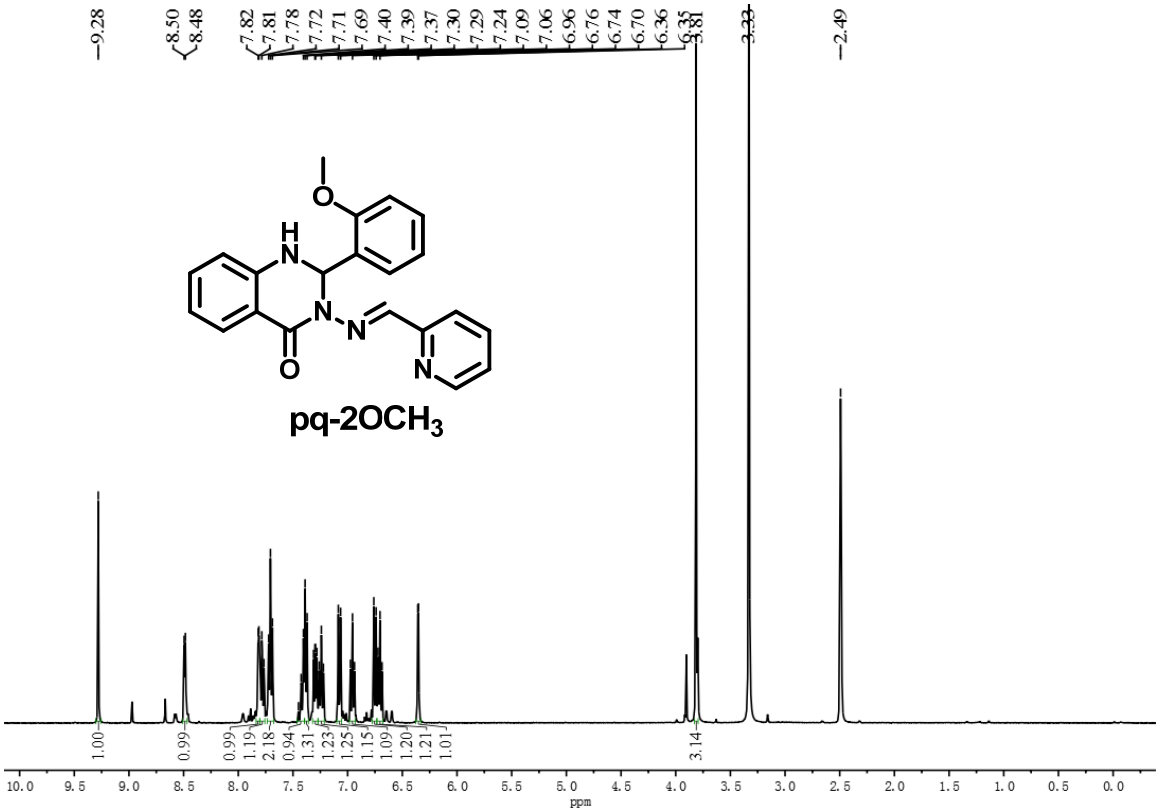

Figure S3. ^{1}H NMR spectrum of **pq-2OCH$_3$** in DMSO.

2-(3-methoxyphenyl)-3-((pyridin-2-ylmethylene)amino)-2,3-dihydroquinazolin-4(1H)-one

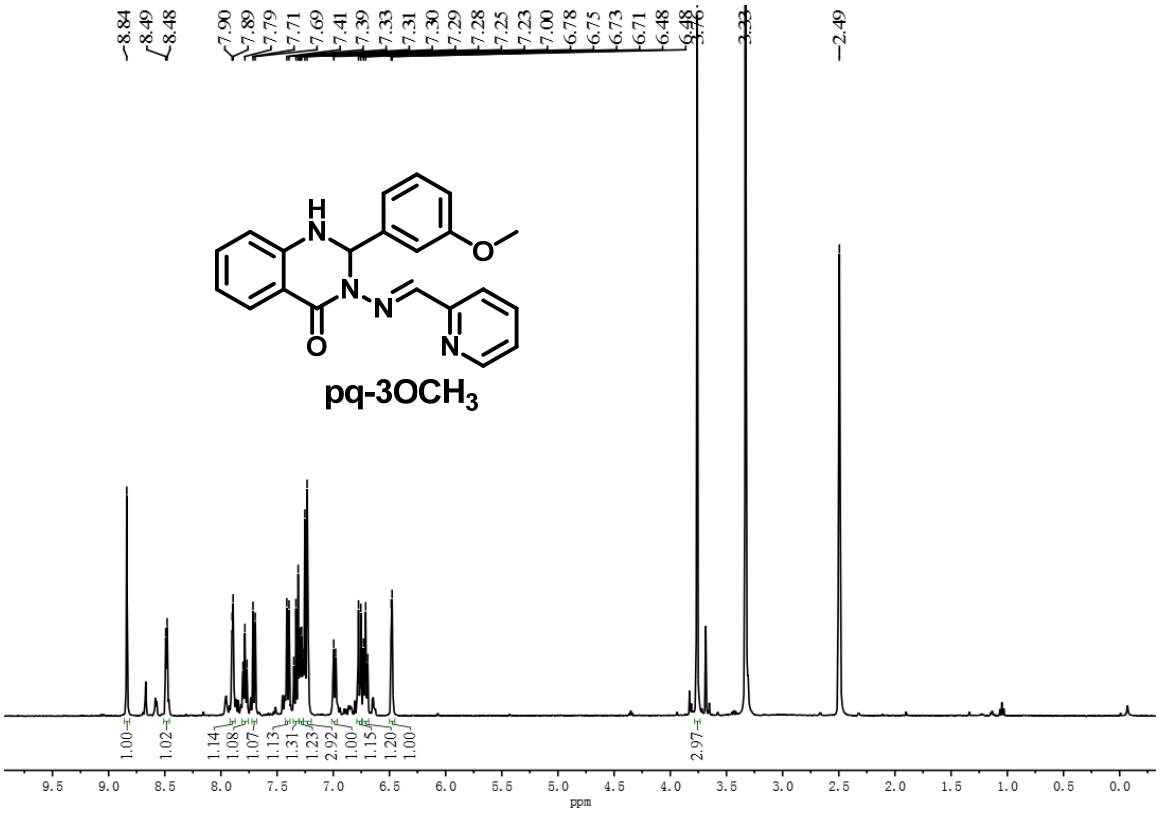

Figure S4. ^{1}H NMR spectrum of **pq-3OCH$_3$** in DMSO.

2. IR Spectroscopy

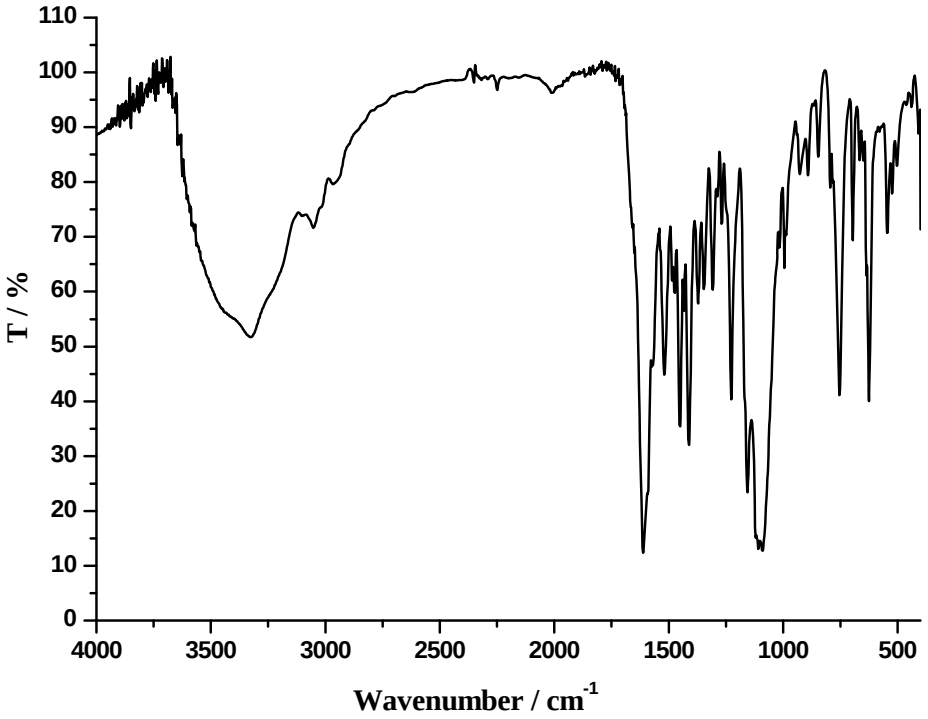

Figure S5. IR spectrum of $[Fe(pq\text{-}2py)_2](ClO_4)_2 \cdot CH_3OH \cdot 2H_2O$ **(1)** at room temperature.

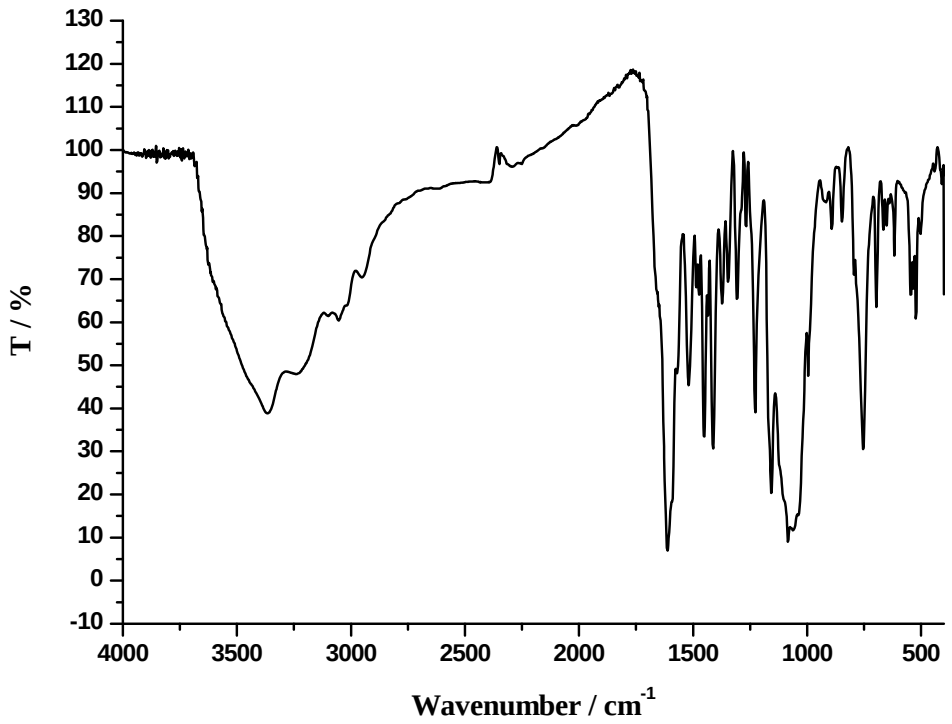

Figure S6. IR spectrum of $[Fe(pq\text{-}2py)_2](BF_4)_2 \cdot 2CH_3CN \cdot 1.75H_2O$ **(2)** at room temperature.

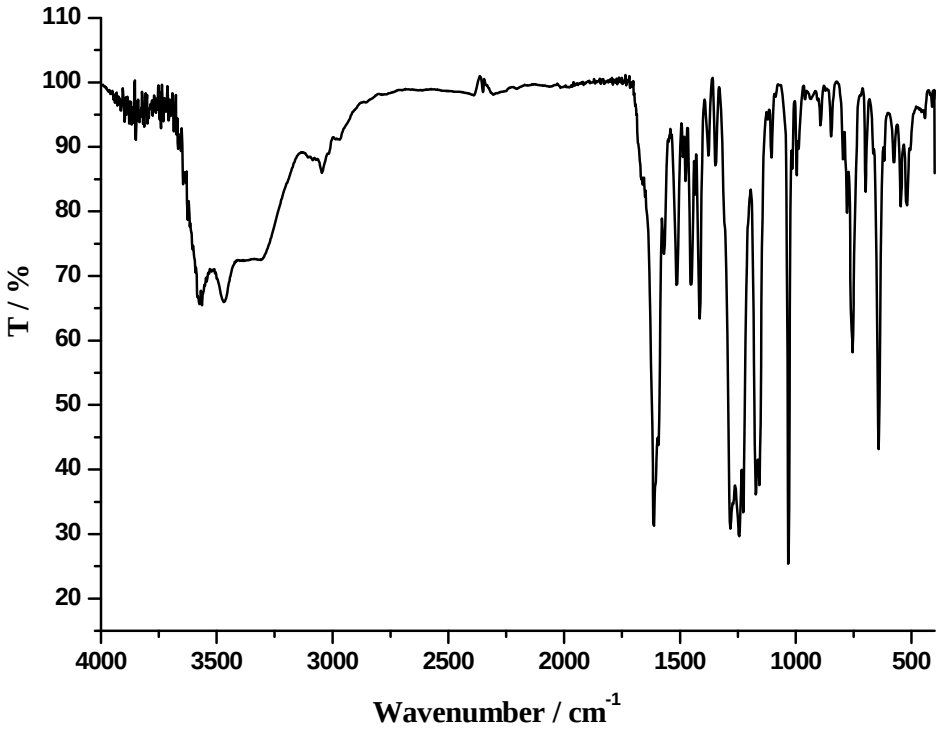

Figure S7. IR spectrum of $[Fe(pq\text{-}2py)_2](CF_3SO_3)_2 \cdot CH_3CN \cdot CH_3OH$ **(3)** at room temperature.

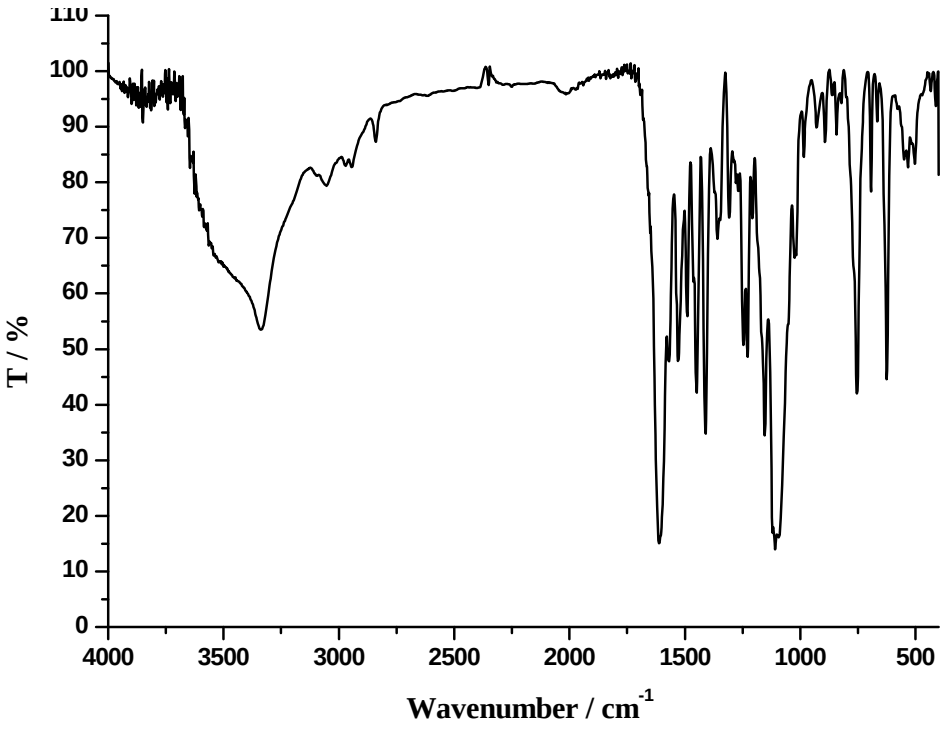

Figure S8. IR spectrum of $[Fe(pq\text{-}2OCH_3)_2](ClO_4)_2 \cdot H_2O$ **(4)** at room temperature.

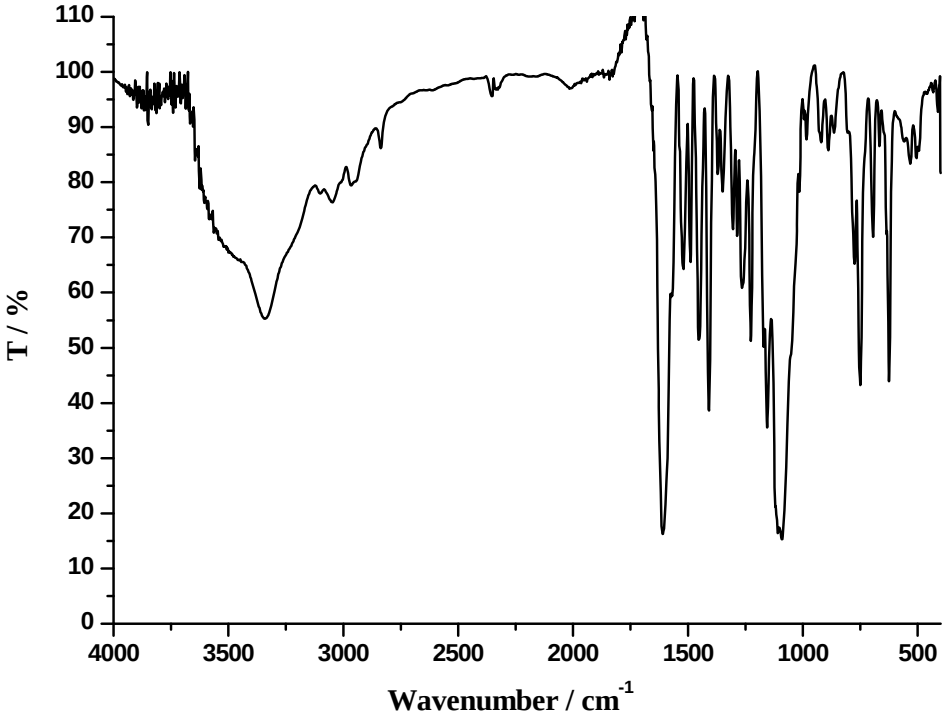

Figure S9. IR spectrum of $[Fe(pq\text{-}3OCH_3)_2](ClO_4)_2 \cdot H_2O$ **(5)** at room temperature.

(a)

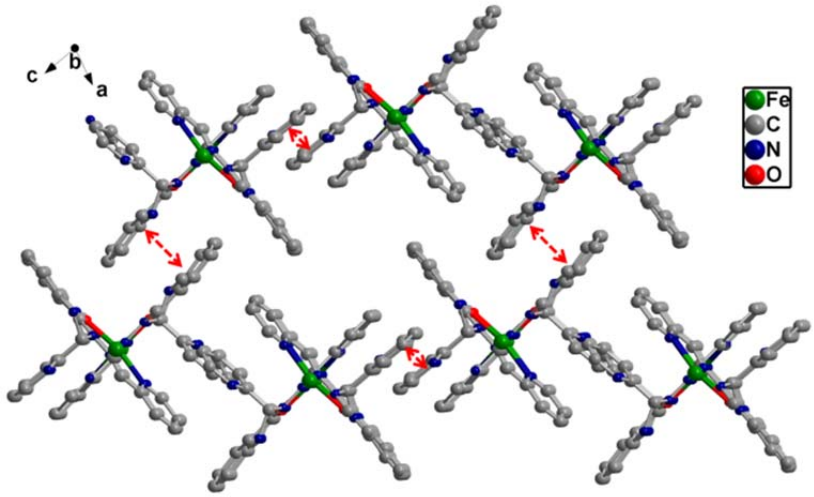

(b)

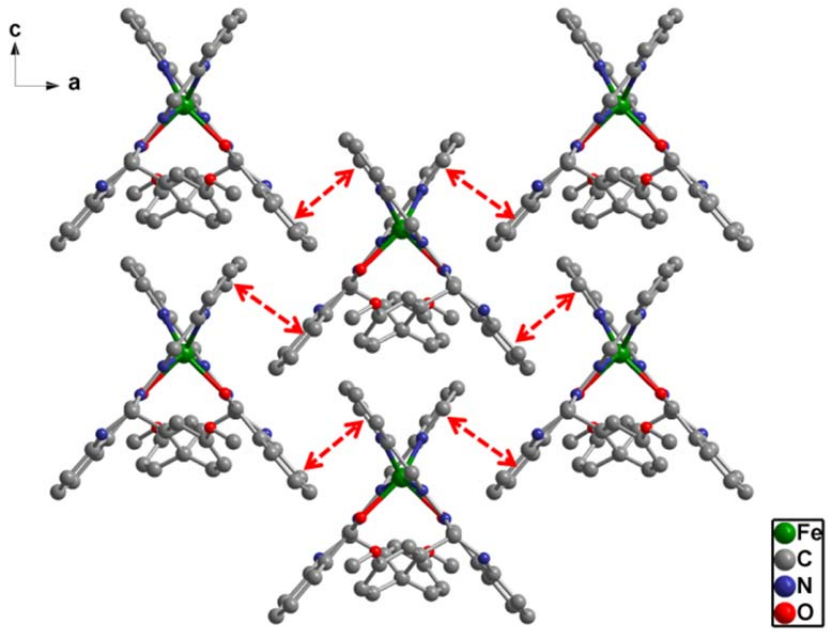

Figure S10. Crystal packing portion of the crystal structure of **2** (100 K, a) and **3** (200 K, b) at, as viewed along the crystallographic *b* axis, highlighting the intermolecular π…π stacking.

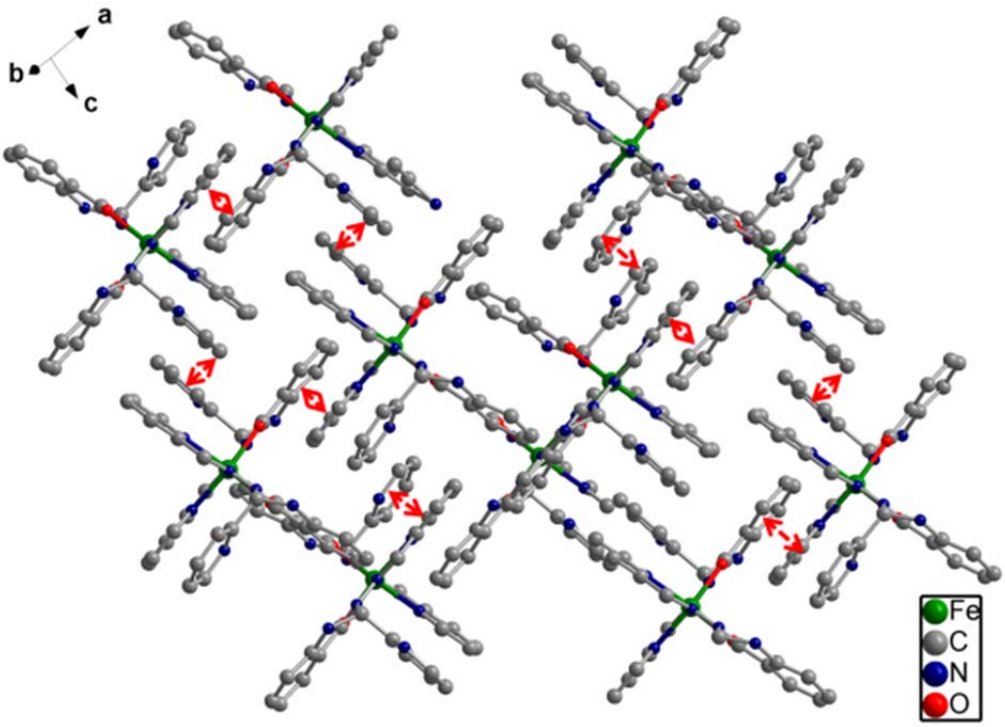

Figure S11. Crystal packing portion of the crystal structure of **5** as viewed along the crystallographic *b* axis, highlighting the intermolecular π…π stacking.

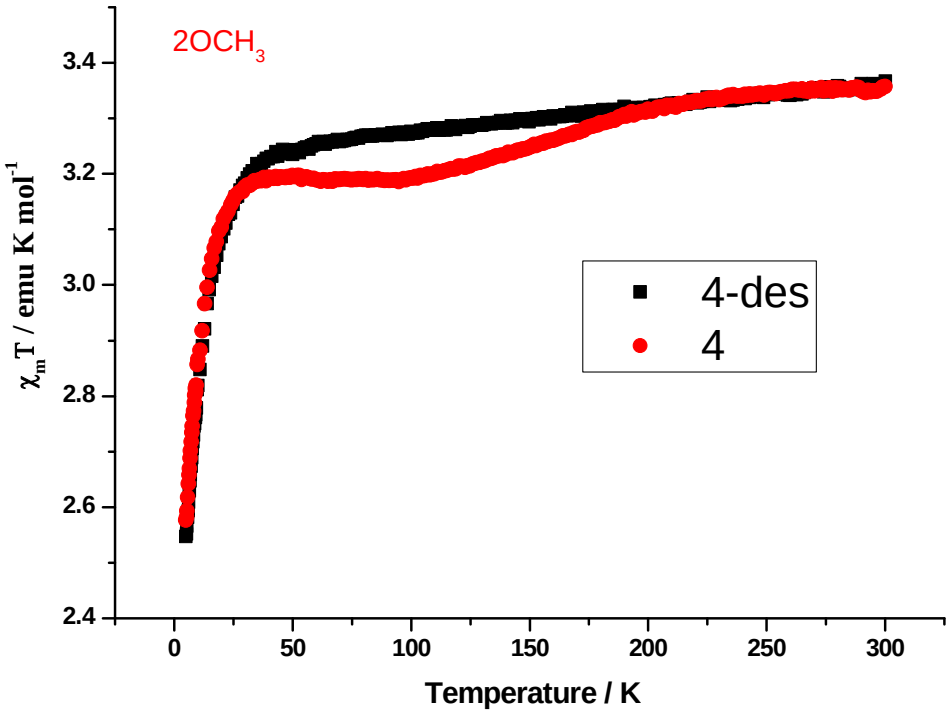

(a)

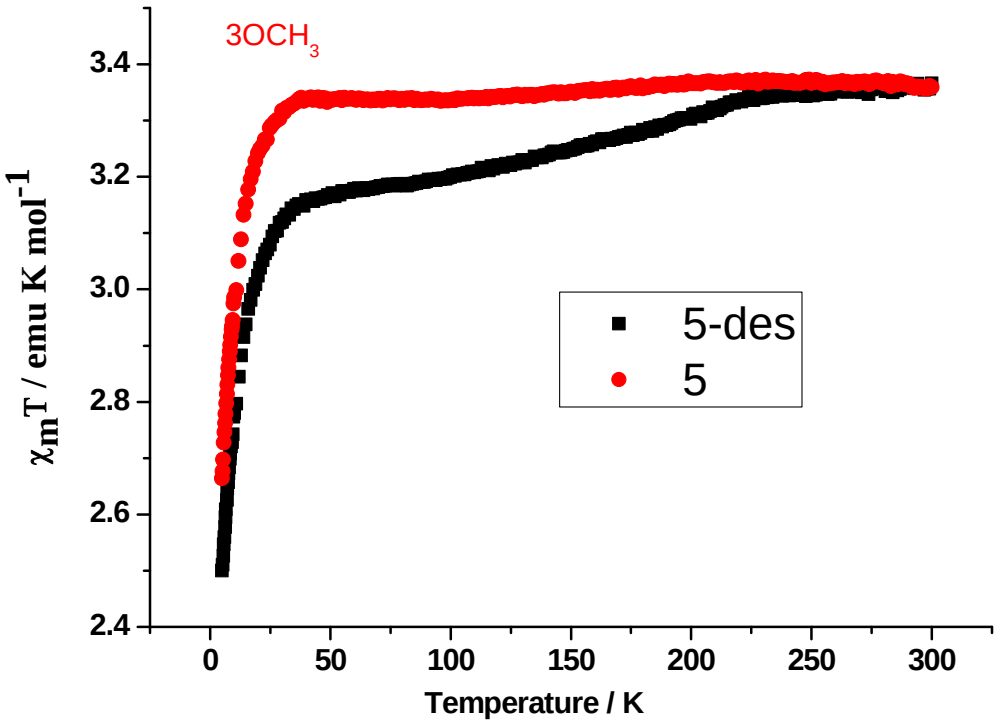

(b)

Figure S12. (a) Plots of $\chi_m T$ versus T for compounds **4**, **5** and their corresponding desolvated samples.

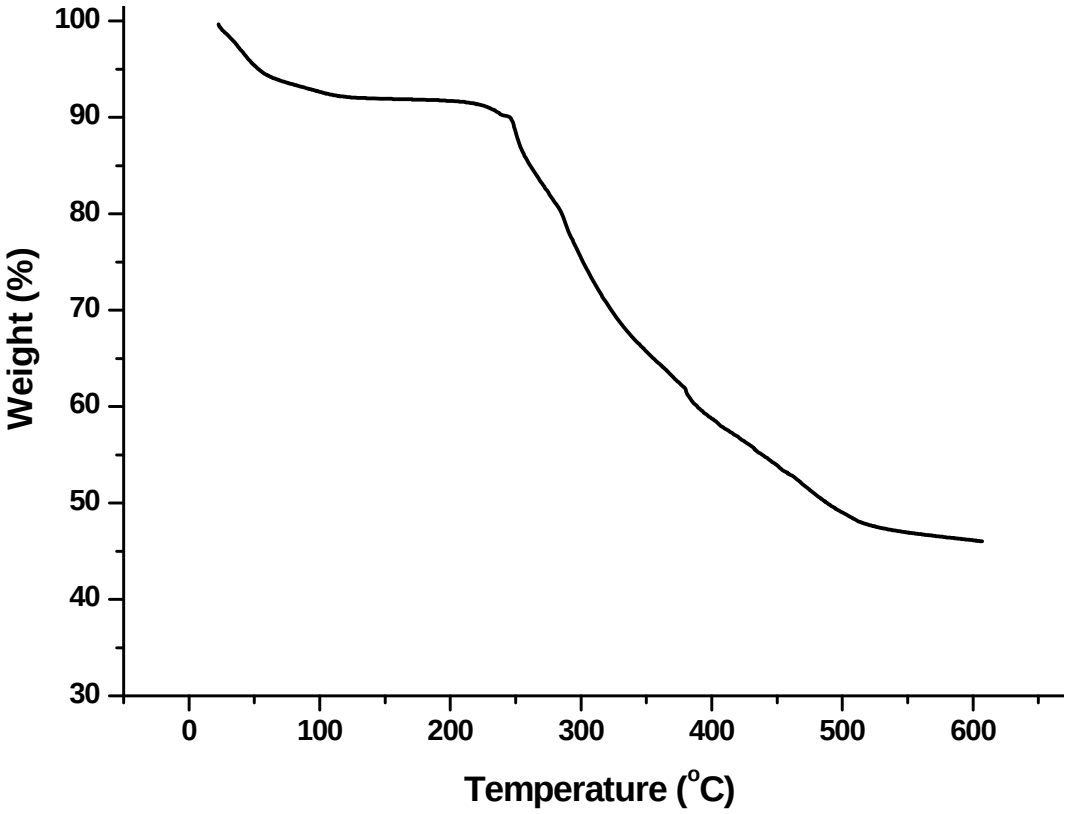

Figure S13. TGA curves of complex $[Fe(pq\text{-}2py)_2](BF_4)_2 \cdot 2CH_3CN \cdot 1.75H_2O$ **(2)** .

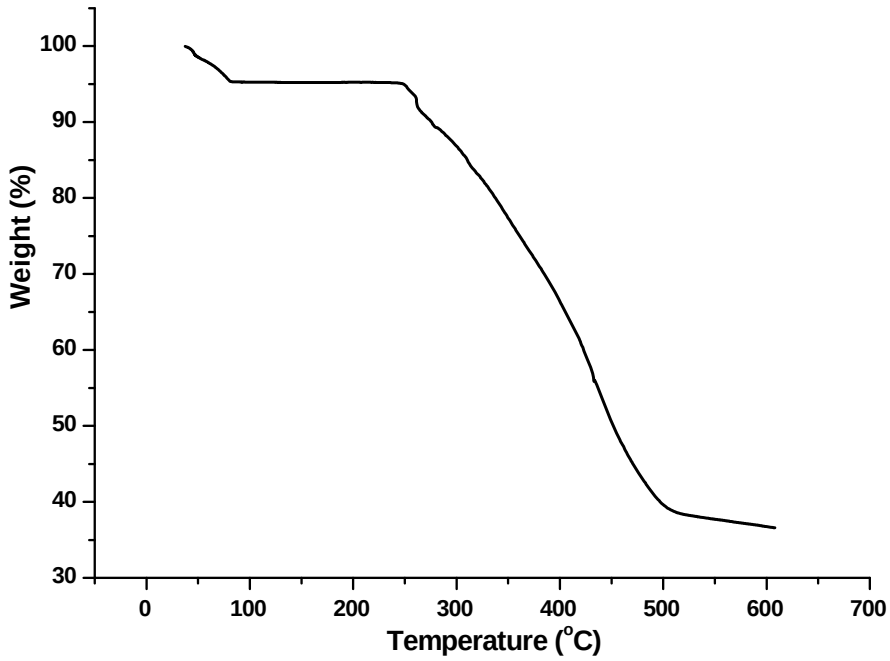

Figure S14. TGA curves of complexe $[Fe(pq\text{-}2py)_2](CF_3SO_3)_2 \cdot CH_3CN \cdot CH_3OH$ **(3)**